



Universiteit  
Leiden

The Netherlands

## **Antibiotic Discovery: from mechanistic studies to target ID**

Kotsogianni, A.I.

### **Citation**

Kotsogianni, A. I. (2023, June 20). *Antibiotic Discovery: from mechanistic studies to target ID*. Retrieved from <https://hdl.handle.net/1887/3620917>

Version: Publisher's Version

License: [Licence agreement concerning inclusion of doctoral thesis in the Institutional Repository of the University of Leiden](#)

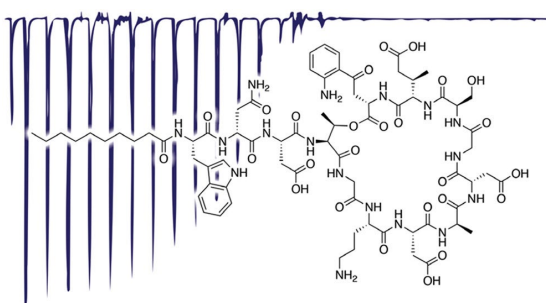
Downloaded from: <https://hdl.handle.net/1887/3620917>

**Note:** To cite this publication please use the final published version (if applicable).

# Chapter 3

## The phospholipid specificity and its role in the calcium-dependent mechanism of action of daptomycin.

**Abstract** | A molecular level understanding of the mechanism of action of antibiotics plays a key role in developing new agents to combat the threat of antimicrobial resistance. Daptomycin, the only clinically used calcium-dependent lipopeptide antibiotic, selectively



disrupts Gram-positive bacterial membranes to elicit its bactericidal effect. In this chapter isothermal titration calorimetry is used to further characterize the structural features of the target bacterial phospholipids that drive daptomycin binding. Our studies reveal that daptomycin shows a clear preference for the phosphoglycerol headgroup. Furthermore, unlike other calcium-dependent lipopeptide antibiotics, calcium binding by daptomycin is strongly dependent on the presence of phosphatidylglycerol. These investigations provide new insights into daptomycin's phospholipid specificity and calcium binding behavior.

Parts of this chapter are published in:

Kotsogianni, I.; Wood, T. M.; Alexander, F. M.; Cochrane, S. A.; Martin, N. I. Binding Studies Reveal Phospholipid Specificity and Its Role in the Calcium-Dependent Mechanism of Action of Daptomycin. *ACS Infect. Dis.*, 7, 2612–2619 (2021).



## 1. Introduction

Daptomycin (**Figure 1**) is the prototypic calcium-dependent lipopeptide antibiotic (CDA).<sup>1</sup> First approved in 2003 for the treatment of complicated skin and skin-structure infections,<sup>2</sup> daptomycin was subsequently approved in 2006 for the treatment of right-sided endocarditis and bacteremia.<sup>3</sup> Daptomycin is generally prescribed as a last resort agent in treating infections due to Gram-positive pathogens including methicillin-resistant and vancomycin-resistant *Staphylococcus aureus* (MRSA & VRSA) and vancomycin-resistant *Enterococci* (VRE). The emergence of daptomycin-resistant phenotypes is consistently linked with alterations in the composition of the bacterial membrane and fortification of the Gram-positive cell-wall.<sup>4</sup> Specifically, daptomycin resistance is often linked to changes related to the bacterial phospholipid phosphatidylglycerol (PG).<sup>5-10</sup> For instance, daptomycin resistance in *S. aureus* is typically associated with mutations in *mprF* (multiple peptide resistance factor), which encodes a bifunctional transmembrane enzyme that performs lysylation of PG,<sup>5,6</sup> effectively masking PG on the membrane. Another daptomycin resistance mechanism reported for *S. aureus* involves the secretion of PG-rich membrane domains. This phenomenon, described as phospholipid shedding,<sup>7</sup> is hypothesized to antagonize the activity of daptomycin by diverting the antibiotic into the extracellular space. Using a related strategy, daptomycin-resistant *Enterococcus faecalis* diverts the antibiotic from the division septum by redistributing cardiolipin-rich domains across its cell membrane.<sup>8</sup> Furthermore, daptomycin resistant mutants have been reported that are able to entirely omit PG and cardiolipin from their phospholipid bilayers, due to loss-of-function mutations in their phospholipid synthases.<sup>9,10</sup>

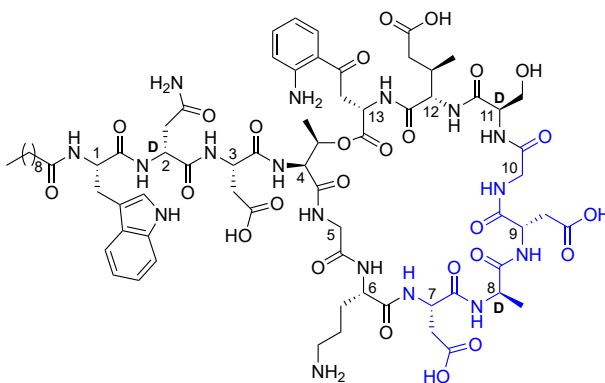


**Figure 1 | Chemical structure of daptomycin** The calcium binding motif Asp-X-Asp-Gly, conserved among the CDAs, is indicated in blue.

The role of PG as a target for daptomycin is further supported by its capacity to antagonize daptomycin's antimicrobial activity *in vitro*.<sup>11</sup> A number of mechanistic studies have also provided insights into the interactions of daptomycin with PG,<sup>12-17</sup> as well as cardiolipin,<sup>18,19</sup> and more recently peptidoglycan precursors.<sup>20</sup> Multiple investigations using a variety of techniques have shown that daptomycin oligomerizes and induces significant changes to vesicles containing PG or PG/cardiolipin mixtures in a calcium dependent manner.<sup>12-15</sup> Recently, a fluorescence microscopy study showed that daptomycin colocalized with PG lipids in giant unilamellar vesicles and subsequently induced formation of daptomycin-PG clusters.<sup>21</sup> Palmer and coworkers have also used Isothermal Titration Calorimetry (ITC) to demonstrate the avidity with which daptomycin binds PG-containing large unilamellar vesicles (LUVs) in the presence of calcium ions.<sup>18,22,23</sup> Numerous biophysical studies have led to a generally accepted model wherein daptomycin is incorporated into a lipid assembly on the target membrane which results in changes in the molecular packing and overall fluidity and permeability of bilayers.<sup>19,24,25</sup> This membrane effect in turn impacts several essential membrane-associated processes such as the regulation of cell division and cell wall synthesis.<sup>26,27,20</sup>

The structure of daptomycin is characterized by a macrolactone consisting of 10 amino acids and an exocyclic linear tripeptide, which is *N*-terminally acylated with decanoic acid. Over the past decade synthetic advances have provided access to structural analogues of daptomycin revealing important Structure-Activity Relationship (SAR) information.<sup>28-31</sup> The lipid tail of daptomycin is indispensable for antibacterial action and it is also known that elongation of the fatty acyl chain enhances daptomycin's activity.<sup>1,32</sup> With regard to the peptide core of daptomycin, a number of structural analogues prepared by Taylor and co-workers as well as our own group and others, have provided important insights.<sup>32-34</sup> Changes to the highly conserved Asp-X-Asp-Gly calcium-binding motif (indicated in blue in **Figure 1**) are poorly tolerated as the side chain carboxylates of the Asp<sup>7</sup> and Asp<sup>9</sup> are assumed to be essential for daptomycin's interactions with Ca<sup>2+</sup>.<sup>32</sup> In addition, the noncanonical amino acids 3-methyl glutamic acid (MeGlu<sup>12</sup>) and kynurenine (Kyn<sup>13</sup>) are also important for full activity.<sup>29</sup> Notable, however, is a recent report describing the synthesis of "kynomycin", a daptomycin analogue featuring an *N*-methylated Kyn<sup>13</sup> residue and showing enhanced antibacterial activity both *in vitro* as well as *in vivo*.<sup>35</sup>

**Exploring daptomycin's phospholipid specificity** This chapter describes the use of ITC to investigate the structural features present in the target phospholipids that are responsible for recognition by daptomycin. Specifically, the binding of daptomycin to

vesicles containing PG or other PG-related phospholipids including cardiolipin, dioleoylphosphatidylserine (DOPS), and dioleoylphosphatidyl-propanol (DOP-propanol) was evaluated, providing insights into the role of the phospholipid headgroup (**Figure 2**).

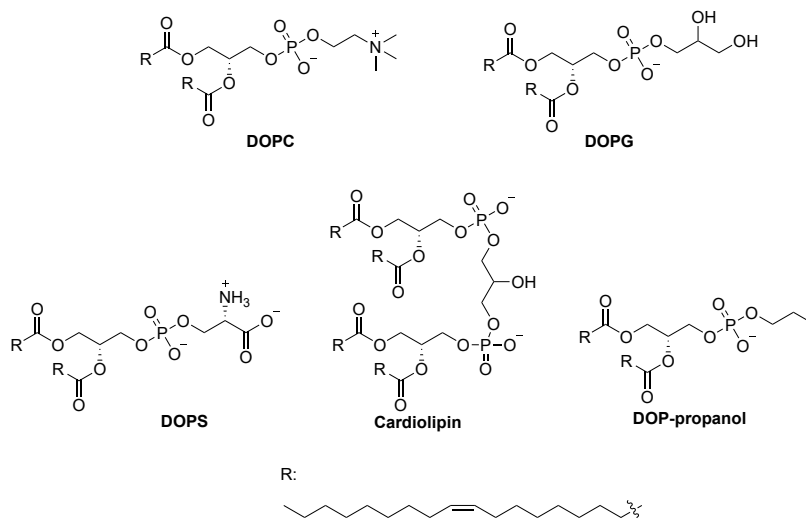


**Figure 2 | Chemical structures of different phospholipids** Negatively charged phospholipids were explored for daptomycin binding. All phospholipids contained the 1,2-dioleoyl-*sn*-glycero-3-phospho motif to allow comparisons between the varying headgroups, namely, choline for DOPC, *rac*-1-glycerol for DOPG, bis-substituted 1,3-glycerol for cardiolipin and 1-propanol for DOP-propanol, and L-serine for DOPS.

## 2. Results and Discussion

**Binding Experiments** The ITC binding experiments were performed using mixed LUVs comprising 25 mol% of the target phospholipid under investigation mixed with 75 mol% dioleoylphosphatidylcholine (DOPC) in buffer containing 5 mM CaCl<sub>2</sub>. All lipids used contained the same 1,2-dioleoyl-*sn*-glycero-3-phospho motif allowing for comparison of the contributions to binding due specifically to the varying headgroups. The most reproducible results were obtained by titrating the vesicle preparations into the ITC sample-cell which contained a solution of daptomycin in the same buffer. **Figure 3** provides examples of representative binding isotherms obtained for each of the different phospholipids evaluated and the results of the titrations are summarized in **Table 1**.

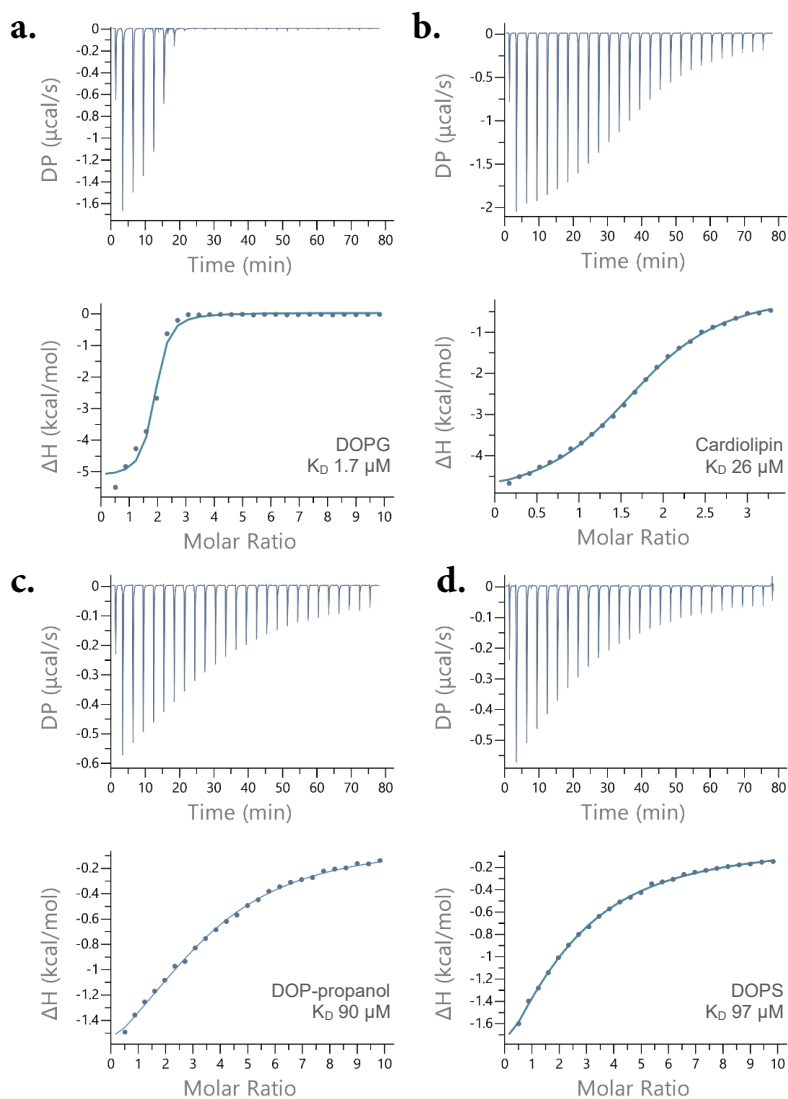


**Figure 3 | Daptomycin interacts with negatively charged phospholipids** Binding isotherms for the titrations of 10 mM DOPC LUVs containing 25 mol% of: **a)** DOPG (titrated into 50  $\mu\text{M}$  daptomycin); **b)** cardiolipin (titrated into 150  $\mu\text{M}$  daptomycin); **c)** DOP-propanol and **d)** DOPS (both titrated into 50  $\mu\text{M}$  daptomycin). The isotherms are representative of three experiments, replicates are shown in **Figure S3, S4, S5 and S6**

**Control Experiments** During the first injections of the binding experiments, where lipid vesicles (1,5  $\mu\text{L}$  per injection) are titrated into daptomycin solution (200  $\mu\text{L}$ ), lipid vesicle–lipopeptide association events might distort the observed enthalpy. Additional control experiments were therefore conducted to ascertain that the enthalpy results are representative of the interactions between binding partners, in contrast with association events (e.g. formation of mixed lipid-peptide micelles or vesicle fusion). The enthalpy associated with the unspecific partitioning/adsorption of the amphiphilic lipopeptide to the lipid bilayers was determined by reverse titration experiments, wherein daptomycin (200  $\mu\text{M}$ ) was titrated into a large excess of the LUV suspensions (1 mM) used in the study. The total enthalpy changes ( $\Delta\Delta\text{H}$ ) obtained were negligible (**Figure S1**) and therefore partitioning/adsorption is considered to not interfere with the measurement. Additional control experiments included LUVs titrations into buffer, and buffer titration into daptomycin solution to determine the dilution heat produced from each binding partner.

**Daptomycin specifically recognizes the glycerol headgroup of phosphoglycerol** In line with expectations,<sup>18</sup> the titration with DOPG-containing LUVs resulted in a strongly exothermic binding isotherm (**Figure 3a**). This binding is attributable to the interaction of daptomycin with DOPG given that no such exothermic signal results from the titration of “blank” LUVs containing 100 mol% DOPC (control titration, **Figure S2**). A dissociation constant ( $K_D$ ) of  $1.7 \pm 0.08 \mu\text{M}$  was thus determined for daptomycin binding to DOPG-containing LUVs using a one-site binding model with the strength of the interaction (determined by the free energy of binding  $\Delta\text{G}$ ) being ruled by an enthalpic contribution (**Table 1**). Building upon these findings we proceeded to assess the binding of daptomycin to the other phospholipids. We next investigated daptomycin’s interaction with cardiolipin, a bisphosphatidyl-glycerol lipid variant common in bacterial membranes.<sup>36</sup> Previous studies have indicated that increased levels of cardiolipin in bacterial membranes may contribute to daptomycin resistance<sup>4</sup> and binding studies with LUVs containing mixtures of PG and cardiolipin indicate that daptomycin does interact with cardiolipin.<sup>18</sup> Given that cardiolipin contains a second 1,2-dioleoyl-*sn*-glycero-3-phosphate moiety in place of one of the hydroxyl groups found in PG, additional ionic interactions with daptomycin are possible. Of note, the additional phosphatidate present in cardiolipin does not appear to increase the negative net charge



**Table 1. Thermodynamic parameters for daptomycin binding anionic membranes by ITC.**

Phospholipid <sup>a</sup>	K <sub>D</sub> (μM)	N (sites)	ΔH (kcal/mol)	-TΔS (kcal/mol)	ΔG (kcal/mol)
DOPG <sup>b</sup>	1.72 ± 0.08	1.72 ± 0.03	-5.26 ± 0.05	-2.60 ± 0.04	-7.86 ± 0.03
Cardiolipin <sup>c</sup>	26.23 ± 1.35	1.81 ± 0.04	-4.98 ± 0.11	-1.25 ± 0.11	-6.23 ± 0.01
DOP-propanol <sup>b</sup>	90.00 ± 1.90	ND	ND	ND	-5.52 ± 0.01
DOPS <sup>b</sup>	97.00 ± 19.71	ND	ND	ND	-5.49 ± 0.12

<sup>a</sup>LUVs (10 mM, 25 mol% phospholipid:75 mol% DOPC) were titrated into the ITC sample cell containing daptomycin at <sup>b</sup>50 μM or <sup>c</sup>150 μM, in 5 mM CaCl<sub>2</sub>, 20 mM HEPES, 150 mM NaCl, pH 7.4. The results shown are the average of three experiments with the standard deviation indicated. ND: For binding of daptomycin to DOP-propanol and DOPS, reliable values for N, ΔH, and -TΔS could not be determined due to the shape of the isotherms obtained under the experimental conditions used.

of the LUV suspensions; the zeta potential of 25 mol% DOPG LUVs is of the same magnitude as the corresponding cardiolipin LUVs, as assessed by electrophoretic light scattering (**Table S1**). As illustrated in **Figure 3b**, a clear interaction is observed when cardiolipin-containing LUVs are titrated into daptomycin with a corresponding K<sub>D</sub> value of 26.23 ± 1.35 μM. This binding is at least 15-fold weaker than that measured for DOPG and suggests that the presence of an additional negatively charged phosphatidic acid moiety does not compensate for the concomitant loss of a hydrogen bond donor.

These findings indicate that the calcium-dependent interaction of daptomycin with phospholipid headgroups is dependent on the availability of the hydrogen bonding interactions provided by both glycerol hydroxyl groups. In the case of cardiolipin-containing mixed membranes, the presence of just one 2'-hydroxyl group may therefore not suffice for inducing daptomycin to adopt its fully active conformation. This rationale is also in line with the finding that high cardiolipin content in PG/PC bilayers prevents the characteristic daptomycin-mediated membrane disruption<sup>18</sup> an observation which was also recently corroborated by investigations performed with atomic force microscopy.<sup>24</sup>

To further investigate the contribution of hydrogen bonding and electrostatic interactions to daptomycin's affinity for phospholipids we next assessed its binding to LUVs containing dioleoylphosphatidyl-propanol (DOP-propanol) and the naturally occurring anionic phospholipid dioleoylphosphatidylserine (DOPS).<sup>36</sup> While DOP-propanol contains the same aliphatic backbone as DOPG, it lacks both hydroxyl groups of the glycerol moiety. This results in a significant loss of binding affinity with a measured K<sub>D</sub> value of 90.00 ± 1.90 μM (**Figure 3c**). In the case of DOPS the glycerol motif is replaced by a serine residue linked via its hydroxyl side chain to the 1,2-dioleoyl-*sn*-

glycero-3-phosphate moiety. Thus, while DOPS lacks the two hydroxy groups of the glycerol moiety, it does contain a zwitterionic amino acid unit. These additional charged amino and carboxylate functionalities do not, however, compensate for the missing hydroxyl groups and in fact further reduce daptomycin's affinity for the DOPS-containing LUVs, with an associated  $K_D$  value of  $97.0 \pm 19.7 \mu\text{M}$  (**Figure 3d**). Collectively, our analyses reveal the specific role of the glycerol moiety in the recognition of PG by daptomycin. These findings are well in line with the commonly accepted model describing the colocalization of daptomycin with PG-rich membrane domains in vesicles<sup>21,19</sup> and in bacterial cells.<sup>20,26,23</sup>

**Investigating lipid II binding** Bacterial membrane regions rich in PG and cardiolipin also typically contain the machinery for cell wall biogenesis.<sup>26,27,37</sup> While previous studies have suggested that daptomycin interferes with cell wall synthesis,<sup>26,27</sup> a recent report from Schneider and coworkers provides evidence for a direct interaction of daptomycin with the cell wall building block lipid II and its precursors undecaprenyl phosphate ( $C_{55}\text{-P}$ ) and undecaprenyl pyrophosphate ( $C_{55}\text{-PP}$ ).<sup>20</sup> Using a range of biochemical assays, the interaction of daptomycin with these cell wall precursors was shown to be dependent on the presence of  $\text{Ca}^{2+}$  ions and PG. Given our group's previous success in using ITC to assess lipid II binding to peptide antibiotics including nisin<sup>38</sup> and teixobactin<sup>39</sup> (further applications outlined in **Chapter 2**), we were curious to see if a similar approach could be used to characterize the interaction of daptomycin with lipid II. To do so, we prepared LUVs containing a range of lipid II (1-2 mol%) and DOPG (1-20 mol%) concentrations and titrated them into solutions containing daptomycin. However, despite investigating a variety of conditions, we were not able to detect any measurable differences relative to the titrations performed using DOPG-containing LUVs lacking lipid II. A possible explanation is that the heat produced by the interaction of daptomycin with PG effectively drowns out any heat signal due to lipid II binding (**Figure 4**).

In an attempt to isolate the lipid II effect from the heat associated with daptomycin's interaction with PG, mixed DOPG/DOPC LUVs containing 2 mol% lipid II were titrated into a premixed solution of daptomycin and DOPG, but this also failed to produce any measurable signal (**Figure 5a**). As a positive control we performed the same binding experiment with nisin in place of daptomycin. When DOPG/DOPC LUVs containing 2 mol% lipid II are titrated into a mixture of nisin and DOPG, binding is readily detected (**Figure 5b**). These results suggest that nisin binds lipid II more tightly than daptomycin, a finding in keeping with previously reported antagonization studies performed with both antibiotics: it is in fact known that PG antagonizes the activity of daptomycin<sup>11</sup> while

lipid II does not.<sup>40</sup> Conversely, for nisin, the addition of lipid II very effectively antagonizes its antibacterial activity.<sup>40</sup> We are careful to note that while our results do not provide evidence for lipid II binding by daptomycin, this may also reflect a limitation of the ITC based methods used to study the interaction.

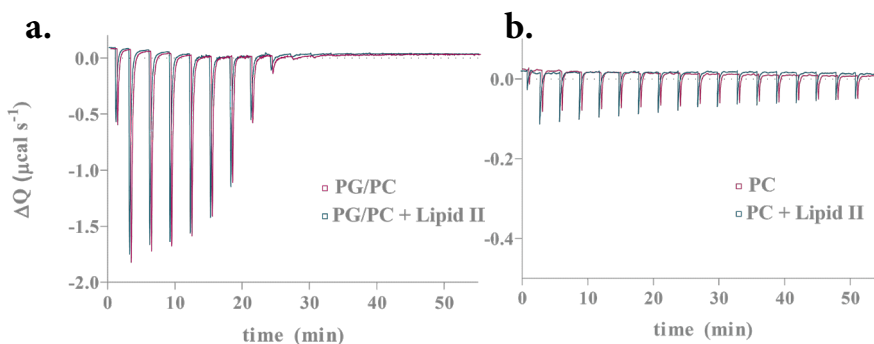


**Figure 4 | Lipid II content does not influence vesicle interactions to daptomycin** Stacked thermograms for the titrations of DOPG-containing LUVs with (magenta) and without (cyan) lipid II into daptomycin in the presence of 5 mM  $\text{CaCl}_2$ . The binding of DOPG drowns out any possible interaction with lipid II. Total lipid 10 mM plus: a) 20 % DOPG  $\pm$  1 % lipid II into 100  $\mu\text{M}$  daptomycin and b) 100 % DOPC  $\pm$  1 % lipid II into 50  $\mu\text{M}$  daptomycin, only heat of dilution is observed in absence of PG.

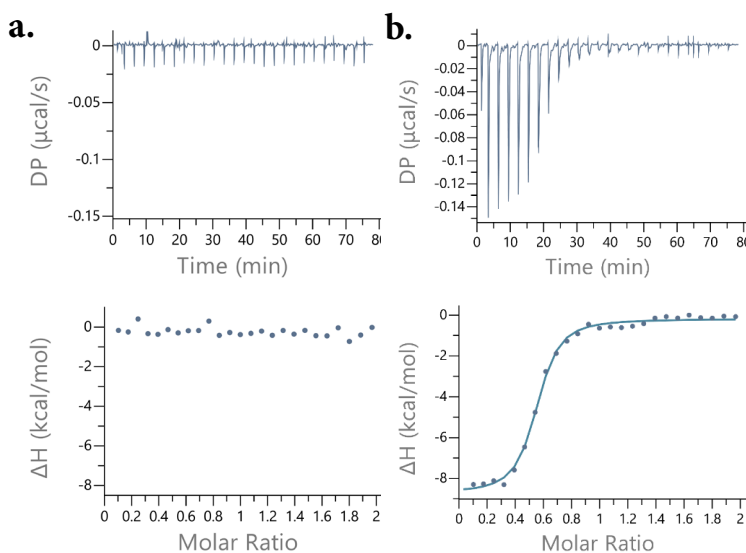


**Figure 5 | Titrations of LUVs containing 2 mol% lipid II and 20 mol% DOPG in DOPC (10 mM) into a solution of: a) 20  $\mu\text{M}$  daptomycin, 2 mM DOPG or b) 20  $\mu\text{M}$  nisin, 2 mM DOPG. In both cases the buffer used consisted of 20 mM HEPES, 5 mM  $\text{CaCl}_2$ , 150 mM NaCl, pH 7.4.**

**Calcium dependency** We also performed a series of ITC investigations to characterize the binding of  $\text{Ca}^{2+}$  by daptomycin in comparison to another well-characterized CDA, laspartomycin C (**Figure 6a**). To date, laspartomycin C is the only CDA for which a crystal structure has been solved that shows the lipopeptide in complex with both  $\text{Ca}^{2+}$  and its target phospholipid ( $\text{C}_{55}\text{-P}$ ).<sup>11</sup> This crystal structure clearly reveals how the Asp-X-Asp-Gly calcium-binding motif and the phospholipid both participate in the binding of two calcium ions. In line with previously reported Circular Dichroism (CD) studies,<sup>11</sup> titration of  $\text{Ca}^{2+}$  into laspartomycin C alone generated a clear exothermic signal (**Figure 6b**).

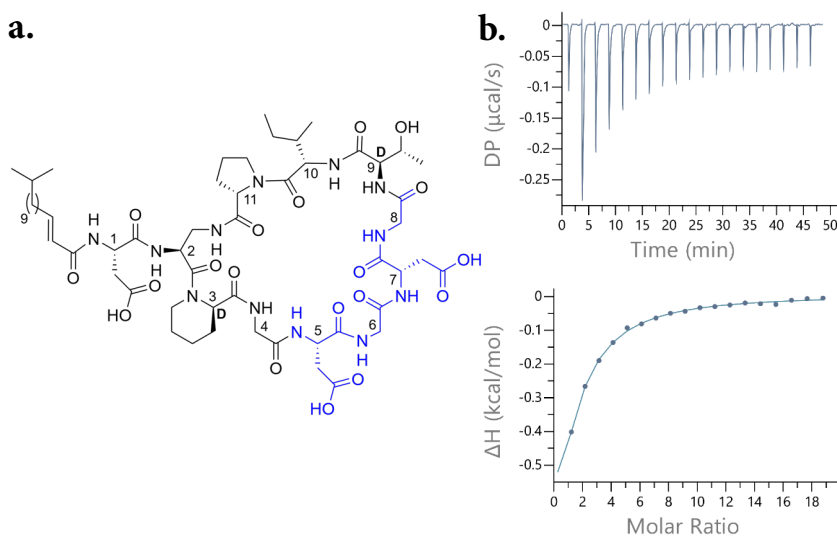


**Figure 6 | Laspartomycin C forms a complex with calcium ions** a) Structure of laspartomycin C with calcium binding motif highlighted in blue and b) thermogram resulting from titration of 5 mM  $\text{CaCl}_2$  into 50  $\mu\text{M}$  laspartomycin C. Representative of three experiments, replicates are shown in **Figure S9**.

In contrast with the above-described results, titration of  $\text{CaCl}_2$  into daptomycin alone gave no indication of binding. The unexpected difference in the calcium binding behavior of these two CDAs, indicates that, despite sharing the conserved  $\text{Ca}^{2+}$  binding motif, the structural differences between laspartomycin C and daptomycin significantly impact their ability to bind  $\text{Ca}^{2+}$ . In a follow-up experiment we found that, when a solution of  $\text{CaCl}_2$  was titrated into a mixture of daptomycin and PG-containing vesicles, a significant exothermic signal is produced (**Figure 7**). We further demonstrated that this heat is produced as a result of complex formation between all the three components: daptomycin, PG, and  $\text{Ca}^{2+}$ , as no appreciable signal was detected when  $\text{CaCl}_2$  was titrated

into PG-vesicles, or neutral DOPC vesicles (**Figure 7**). These findings are in agreement with recent studies utilizing fluorescence microscopy<sup>21</sup> and CD methods<sup>16,17</sup> which also indicate that daptomycin's capacity to undergo the conformational changes needed to interact with target membranes is explicitly dependent on the presence of both  $\text{Ca}^{2+}$  and PG.

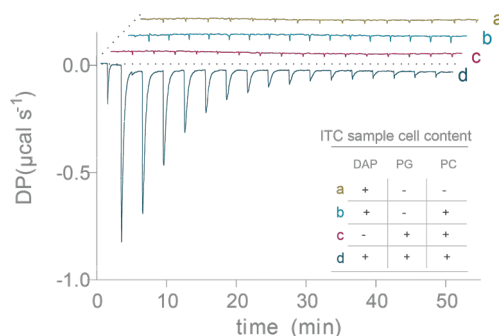


**Figure 7 | Daptomycin does not interact with free calcium ions in solution** Calcium binding daptomycin-PG. The stacked thermograms show the heat exchange upon the 16 first injections of 5 mM  $\text{CaCl}_2$  into the ITC sample cell containing **a**) 50  $\mu\text{M}$  daptomycin (**DAP**) **b**) DAP with DOPC LUVs, **c**) DOPG/DOPC LUV suspension free of antibiotic, or **d**) DAP with DOPG/DOPC LUV suspension. Thermograms are representative of two experiments (**Figure S7** and **S8**, thermodynamic parameters are reported in **Table S2**).

As an extension of the binding studies illustrated in **Figure 2** and summarized in **Table 1**, we also examined the impact of calcium ion concentration on the measured affinity of daptomycin for the different phospholipids evaluated in the present study. This revealed a clear effect wherein elevated  $\text{Ca}^{2+}$  concentration enhanced the measured binding of daptomycin to PG, cardiolipin, DOP-propanol, and DOPS, while reduced calcium ion concentrations had the inverse effect (**Table 2**).

**Table 2.** Effect of calcium content on the dissociation constants of daptomycin binding anionic phospholipids, as measured by ITC.

$[\text{Ca}^{2+}]$ mM	$K_D$ ( $\mu\text{M}$ )			
	DOPG <sup>a</sup>	Cardiolipin <sup>b</sup>	DOP-Propanol <sup>a</sup>	DOPS <sup>a</sup>
0	NB	NB	NB	NB
1	$6.74 \pm 0.21$	$85.17 \pm 8.68$	NB	NB
5	$1.72 \pm 0.08$	$26.23 \pm 1.35$	$90.00 \pm 1.90$	$97.00 \pm 19.71$
10	$1.54 \pm 0.10$	$13.70 \pm 1.08$	$39.73 \pm 5.27$	$49.77 \pm 0.66$

Conditions: 20 mM HEPES, 150 mM NaCl, pH 7.4, LUV formulations titrated into daptomycin at: <sup>a</sup>50  $\mu\text{M}$  or <sup>b</sup>150  $\mu\text{M}$  daptomycin. The results are shown as the average of three experiments with the standard deviation indicated. NB: No binding.

### 3. Conclusions

In conclusion, this chapter provides a comprehensive ITC study that further clarifies the parameters required for phospholipid binding by daptomycin and highlights the importance of these phospholipid partners for calcium ion binding. Our results reveal the optimal nature of the PG phospholipid headgroup and the key role of both hydroxyl group moieties for tight binding.

Also, a recent report indicating a role for the bacterial cell wall precursor lipid II as a target for daptomycin prompted us to study this binding interaction by ITC. While clear lipid II binding was evident in titrations with nisin, a well characterized lipid II binding lanthipeptide, the same approach failed to provide a detectable signal for daptomycin suggesting that ITC methods may not be suitable for characterizing the daptomycin-lipid II interaction. Investigations into the daptomycin's ability to directly bind  $\text{Ca}^{2+}$  also highlight notable differences among structurally related CDAs: while laspartomycin C binds  $\text{Ca}^{2+}$  in the absence of any added phospholipid, for daptomycin the interaction with  $\text{Ca}^{2+}$  is dependent on the presence of phospholipids, with PG providing the greatest effect. Collectively our investigations provide new insights into the way daptomycin binds to its targets and functions as an antibiotic.

### 4. Materials and Methods

**Reagents and materials** Buffers and salts were of ACS reagent grade and were purchased from Carl Roth GmbH (Karlsruhe, Germany) and VWR International (Leuven, Belgium). The phospholipids 1,2-dioleoyl-*sn*-glycerol-3-phosphocholine (DOPC), 1,2-dioleoyl-*sn*-glycerol-3-phospho-*rac*(1-glycerol) (DOPG), 1',3'-bis[1,2-oleoyl-*sn*-glycerol-3-phospho]-glycerol (cardiolipin), 1,2-dioleoyl-*sn*-glycerol-3-phosphopropanol (DOP-propanol), 1,2-dioleoyl-*sn*-glycerol-3-phospho-L-serine (DOPS) were purchased from Sigma-Aldrich (Taufkirchen, Germany). The antibiotic daptomycin (Cubicin, TRX, Toronto, Canada), was used as purchased, nisin (nisinZ, Handary S.A., Brussels, Belgium) was purified according to published procedure<sup>41</sup> before use. Laspartomycin C and Gram-positive lipid-II (lipid II-L-Lys<sup>3</sup>) were obtained synthetically according to published procedures.<sup>42-44</sup>

**Formulation of large unilamellar vesicles (LUVs)** Phospholipid stock solutions (10-30 mM) were prepared in chloroform. Gram-positive lipid II stock solutions (0.3-1.0 mM) were prepared in chloroform/methanol 1:1. Appropriate volumes of the stock solutions were mixed and the organic solvents evaporated under a stream of nitrogen at 35-40 °C. The resulting dry lipid films were hydrated with buffer of specified CaCl<sub>2</sub> content (20 mM HEPES, 150 mM NaCl, pH 7.4) and homogenized by 5 cycles of freezing (-196 °C) and thawing (35-40 °C) to produce vesicle suspensions with a final concentration of 10 mM total lipid. The suspensions were passed through 2 opposite directed Whatman™ polycarbonate membranes with a final pore size of 0.2 μm (Sigma Aldrich, Taufkirchen, Germany) 11 times at room temperature with an Avanti mini extruder (Avanti Polar Lipids Inc., Alabaster, Alabama USA) to yield homogeneous (polydispersity index < 0.1) LUV suspensions of ~140 nm hydrodynamic diameter as assessed by dynamic light scattering (DLS) spectroscopy at 25 °C, on a Zetasizer Nano S (Malvern Panalytical Ltd, Malvern, UK) using acrylic low-volume cuvettes (VWR international, Leuven, Belgium). The Zeta potential of DOPG and cardiolipin containing DOPC LUVs formulated in 20 mM HEPES, pH 7.4 were measured using laser Doppler electrophoresis on the same instrument with a zeta dip cell (Malvern Panalytical Ltd, Malvern, UK). Samples were diluted 100-fold before all DLS measurements.

**Isothermal Titration Calorimetry (ITC)** All binding experiments were performed using a MicroCal PEAQ-ITC Automated microcalorimeter (Malvern Panalytical Ltd, Malvern, UK). **Method A:** The samples were equilibrated to 25 °C prior to measurement. The titrations were conducted at 25 °C under constant stirring at 1000 rpm. Each experiment consisted of an initial injection of 0.3 μL followed by 25 separate injections of 1.5 μL into the sample cell of 200 μL. The time between each injection was 180 seconds and the measurements were performed with the reference power set at 5 μcal s<sup>-1</sup> and the feedback mode set at “high.” **Method B:** The samples were equilibrated to 25 °C prior to measurement. The titrations were conducted at 25 °C under constant stirring at 750 rpm. Each experiment consisted of an initial injection of 0.4 μL followed by 18 separate injections of 2.0 μL into the sample cell of 200 μL. The time between each injection was 150 seconds and the measurements were performed with the reference power set at 10 μcal s<sup>-1</sup> and the feedback mode set at “high”.

**ITC procedure for phospholipid binding** LUV suspensions of 2.5 mM anionic lipid 7.5 mM DOPC or 10 mM DOPC in buffer containing 0, 1, 5 or 10 mM CaCl<sub>2</sub> were titrated into daptomycin solution in the same buffer. Daptomycin solutions were prepared from a 2 mM stock in the same buffer which was stored in -20 °C for no more than 5 days prior

to use. Blank titrations included the titration of buffer into daptomycin and LUVs into buffer. The titrations were conducted according to method A described above.

***ITC procedure for calcium binding daptomycin with LUVs*** A solution of 5 mM CaCl<sub>2</sub> in 20 mM HEPES, 150 mM NaCl, pH 7.4 was titrated into a 0.05 mM solution of daptomycin with or without a suspension of 1 mM LUV in the same buffer. Blank titrations included the titration of buffer into daptomycin (0.05 mM) or daptomycin (0.05 mM) with LUV suspension (1 mM) and CaCl<sub>2</sub> (5 mM) into buffer or LUV suspension. The titrations were conducted according to method A described above.

***ITC procedure for calcium binding in solution*** A solution of 5 mM CaCl<sub>2</sub> in 20 mM HEPES, pH 7.4 was titrated into a 0.05 mM solution of daptomycin or laspartomycin C in the same buffer. Blank titrations included the titration of buffer into the test compounds and CaCl<sub>2</sub> into buffer. The titrations were conducted according to method B described above.

***ITC procedure for partition enthalpy of daptomycin into LUVs*** A solution of 200 μM daptomycin in 20 mM HEPES, 150 mM NaCl, 5 mM CaCl<sub>2</sub>, pH 7.4 was titrated into a 1 mM LUV suspension of 250 μM anionic phospholipid and 750 μM DOPC, in the same buffer. Control titrations included the titration of buffer into the test compounds and daptomycin into buffer. The titrations were conducted according to method B described above.

***ITC data analysis*** The calorimetric data obtained was analyzed using MicroCal PEAQ-ITC Analysis Software Version 1.20 (Malvern Panalytical Ltd, Malvern, UK). Blank titrations and dilution data were compared to, but not subtracted from the binding data to avoid error introduction. For titrations using LUVs with different phospholipid compositions, the binding data are fit with the titrant concentration corresponding to that of the specific phospholipid being investigated. ITC data fitting was made based on the “one set of sites” fitting model of the software. The best fit is defined by chi-square minimization. Low affinity (hyperbolic isotherm) curve fitting<sup>45</sup> generates K<sub>D</sub> within 95 % confidence intervals, from which ΔG is calculated. Standard curve (sigmoidal isotherm) fitting generates K<sub>D</sub>, n, ΔH within 95 % confidence intervals, from which ΔG, -TΔS are calculated. Thermodynamic parameters are reported as the average of three experiments with standard deviation.



## Supplementary Tables

**Table S1. Dynamic light scattering result table** Summary of results of the DLS experiments on LUV formulations.

DOPC LUVs containing 25 % lipid:	Diameter (nm)	PDI	Zeta Potential (mV)
DOPG	136 ± 2	<0.09	-38.3 ± 10
Cardiolipin	137.2 ± 0.7	<0.06	-40.3 ± 5
DOPS	137 ± 2	<0.11	ND
DOP-propanol	133.9 ± 2	<0.12	ND

Hydrodynamic diameter and zeta potential are reported as the average of three independent experiments with standard deviation, and the maximum noted polydispersity index (PDI) is reported. LUV: large unilamellar vesicle, DOPC: dioleoylphosphatidylcholine, DOPG: dioleoylphosphatidylglycerol, DOPS: dioleoylphosphatidylserine, DOP-propanol: dioleoylphosphatidylpropanol, ND: not determined.

**Table S2. Thermodynamic parameters table** Calcium binding the pre-mixed daptomycin DOPG-containing LUV suspension.

ITC cell contents	$K_D$ ( $\mu\text{M}$ )	N (sites)	$\Delta G$ (kcal/mol)
Daptomycin - PG 1:5	25.6 ± 0.0	2.49 ± 0.01	-6.27 ± 0.01

5 mM  $\text{CaCl}_2$  titrated into 50  $\mu\text{M}$  daptomycin - 250  $\mu\text{M}$  DOPG - 750  $\mu\text{M}$  DOPC, in 20 mM HEPES, 150 mM NaCl, pH 7.4. The results are shown as the average of two independent experiments with the standard deviation. LUV: large unilamellar vesicle, DOPC: dioleoylphosphatidylcholine, DOPG: dioleoylphosphatidylglycerol,

## Supplementary Figures

### Enthalpy control titrations for daptomycin binding phospholipids

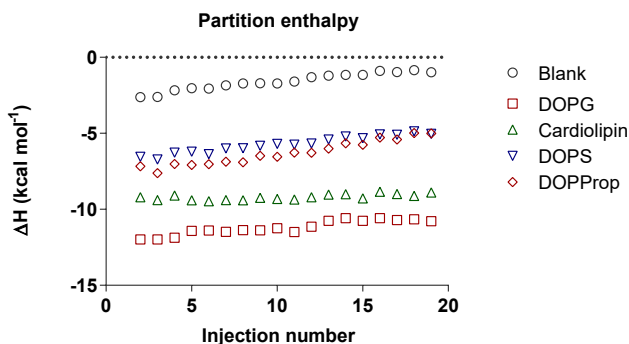


**Figure S1 | Control Partition Enthalpy Measurement** The enthalpy changes that are associated with the unspecific partitioning /adsorption of the amphiphilic lipopeptide to lipid bilayers were determined by a reverse titration experiment, where daptomycin (200 $\mu$ M) is titrated into the LUV suspensions (1 mM) under investigation.

### Thermograms for 100% DOPC LUV titrations

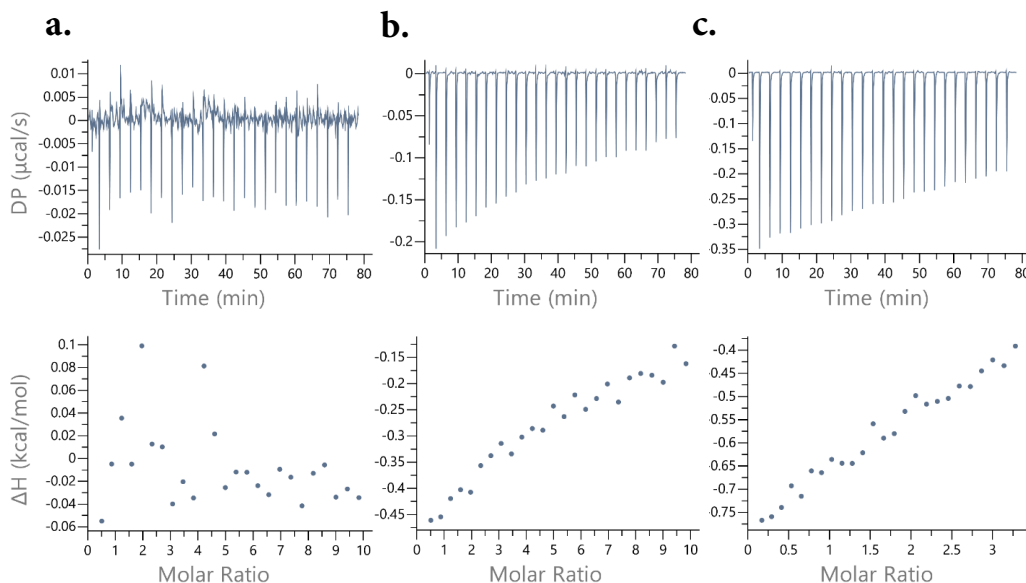


**Figure S2 | Thermograms for 100 % DOPC titrations in the presence of 5 mM CaCl<sub>2</sub>** 10 mM DOPC LUVs titrated into: a) buffer (heat of dilution), b) 50 $\mu$ M and, c) 150  $\mu$ M daptomycin. The heat signal indicates interactions with the membrane phase, however it is too low to fit in a binding model.

## Replicates of Binding Experiments

### Binding thermograms for DOPG titrations

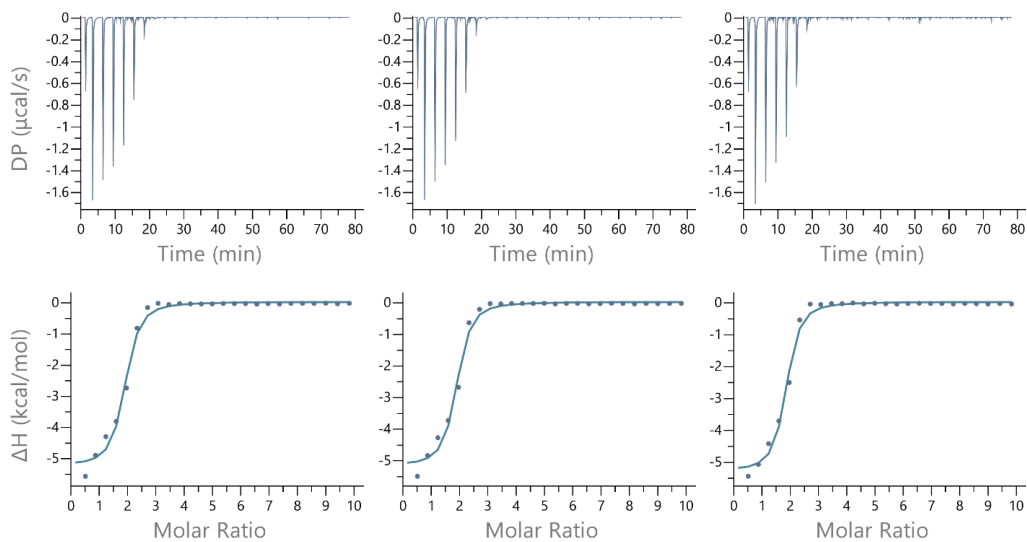


**Figure S3** | Binding isotherms for 25 % DOPG, DOPC LUV titrations into 50  $\mu\text{M}$  daptomycin in 5 mM  $\text{CaCl}_2$ , in triplicate.

### Binding thermograms for cardiolipin titrations

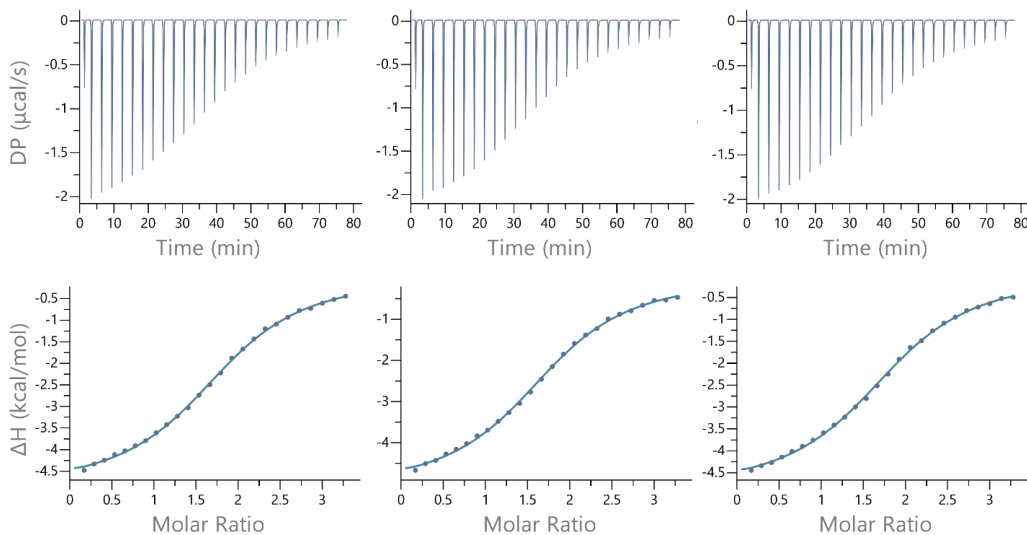


**Figure S4** | Binding isotherms for 25 % cardiolipin, DOPC LUV titrations into 150  $\mu\text{M}$  daptomycin in 5 mM  $\text{CaCl}_2$ , in triplicate.

### Binding thermograms for DOP-propanol titrations

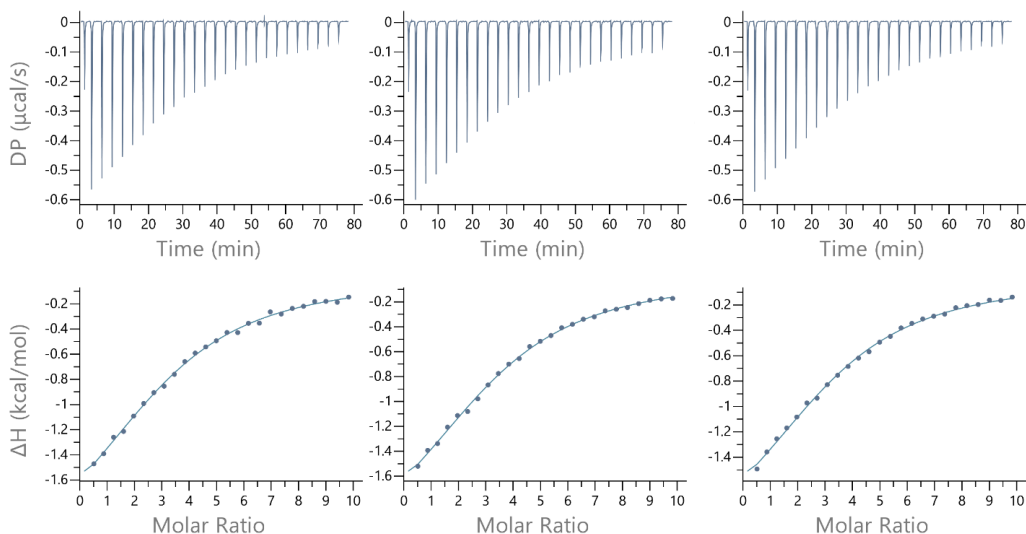


**Figure S5** | Binding isotherms for 25 % DOP-propanol, DOPC LUV titrations into 50  $\mu\text{M}$  daptomycin in 5 mM  $\text{CaCl}_2$ , in triplicate.

### Binding thermograms for DOPS titrations

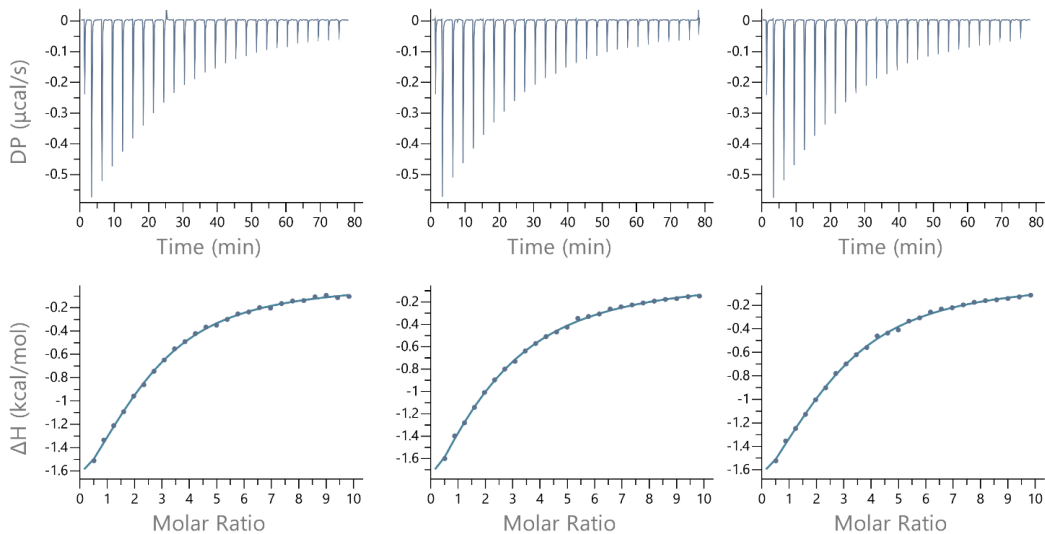


**Figure S6** | Binding isotherms for 25 % DOPS, DOPC LUV (10 mM) titrations into 50  $\mu\text{M}$  daptomycin in 5 mM  $\text{CaCl}_2$ , in triplicate.

### Calcium titrations in LUVs

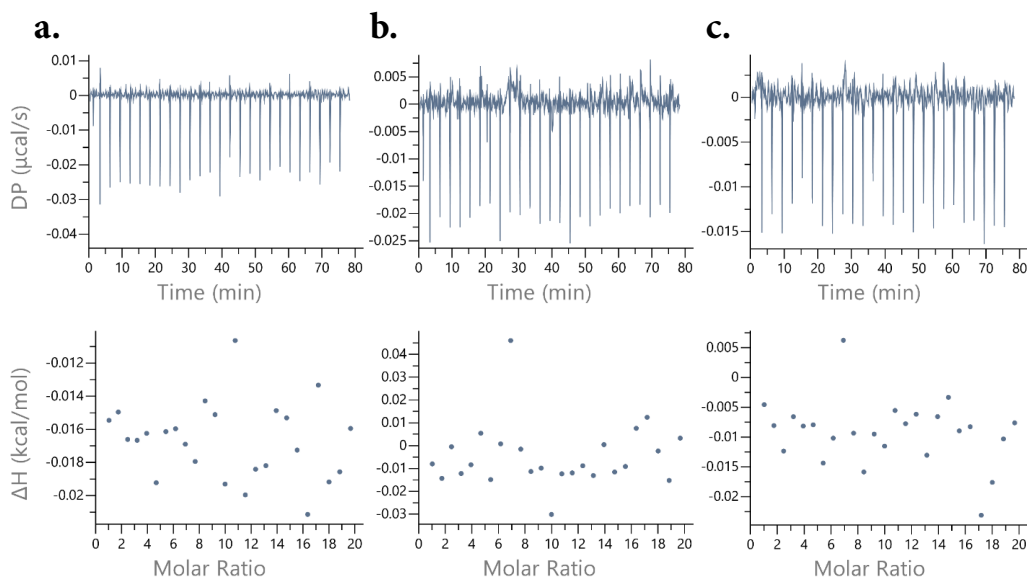


**Figure S7** | Control titrations for  $\text{Ca}^{2+}$  binding. 5 mM  $\text{CaCl}_2$  titrated into **a**) buffer, **b**) 100% DOPC (blank) LUVs (1 mM), **c**) 25% DOPG, DOPC LUVs (1 mM).

### Calcium titrations in daptomycin $\pm$ LUVs

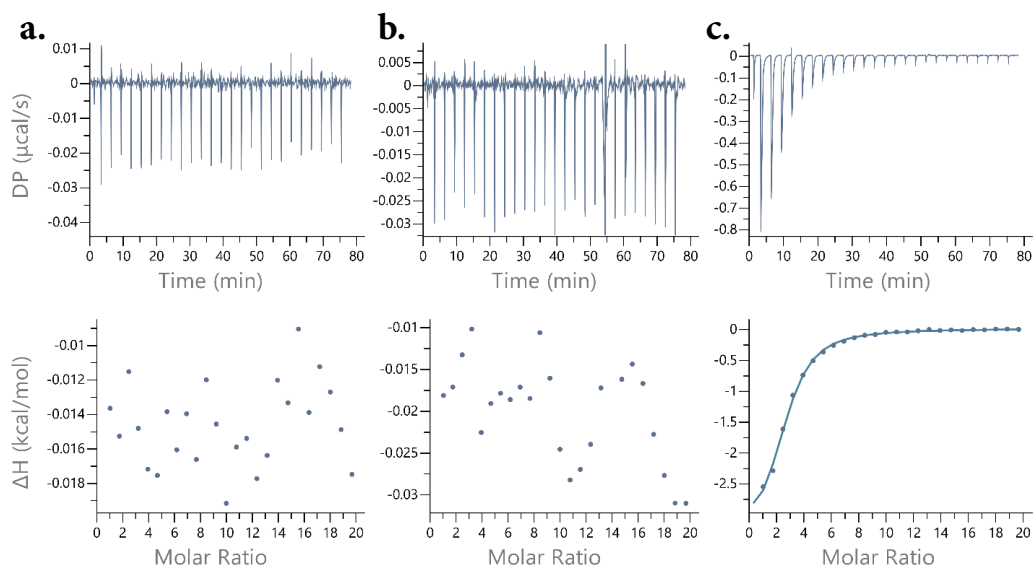


**Figure S8** | Titrations of 5 mM  $\text{CaCl}_2$  into daptomycin 50  $\mu\text{M}$  and **a**) no LUVs present, **b**) 100% DOPC LUVs (1 mM), **c**) 25% DOPG LUVs (1 mM).

### Calcium binding laspartomycin C

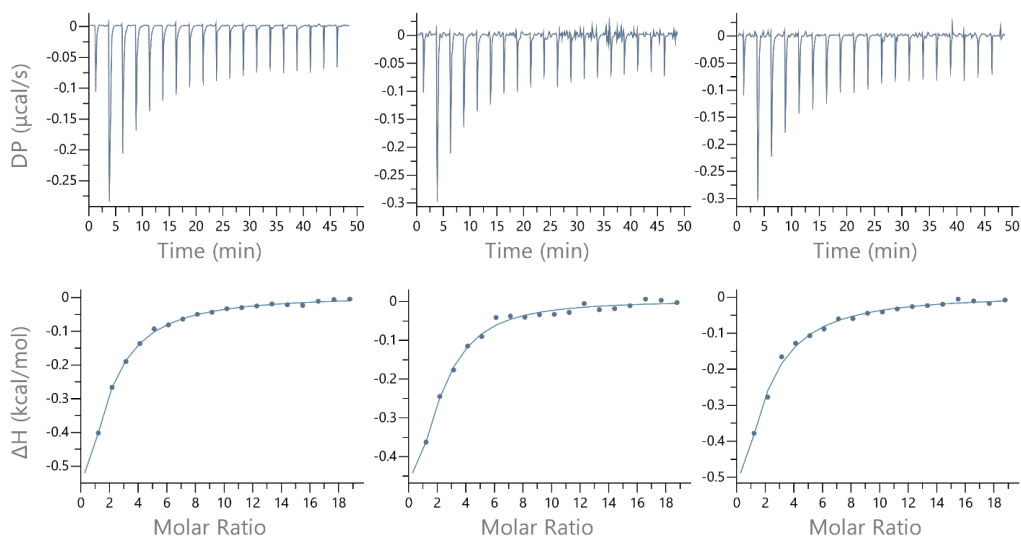


**Figure S9** | Titration of 5mM  $\text{CaCl}_2$  into 50  $\mu\text{M}$  laspartomycin C in triplicate.

### Control thermograms for 25 % DOPG LUVs titrations

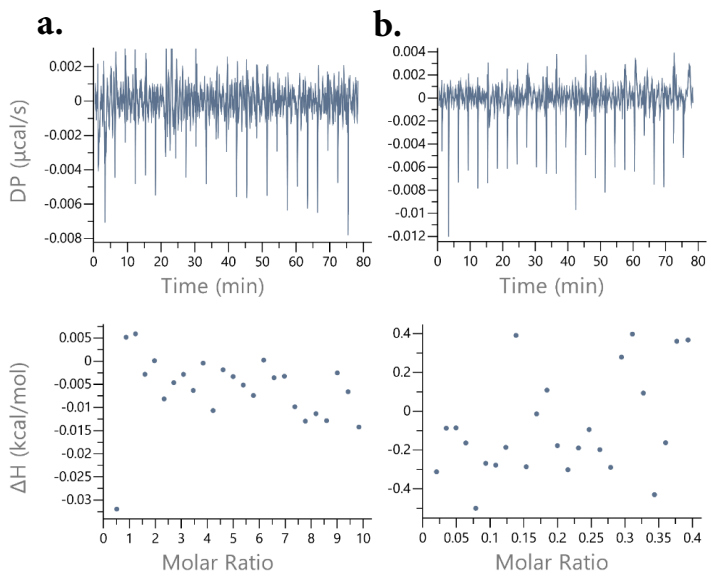


**Figure S10** | Control experiments for DOPG binding in the presence of 5 mM  $\text{CaCl}_2$ . **a**) 25 % DOPG, DOPC LUV (10 mM) titrated into buffer, **b**) buffer titrated into 50  $\mu\text{M}$  daptomycin.

**Acknowledgements** Charlotte M. J. Wesseling is gratefully acknowledged for providing purified nisin, Thomas M. Wood for supplying synthetic laspartomycin C. Francesca M. Alexander and Stephen A. Cochrane synthetically obtained and kindly provided lipid II for this study. Niek S. A. Crone and Roman J. T. Leboux are acknowledged for assistance with DLS experiments.

## References

1. Debono, M. *et al.* Enzymatic And Chemical Modifications Of Lipopeptide Antibiotic A21978C: The Synthesis And Evaluation Of Daptomycin (LY146032). *J. Antibiot. (Tokyo)*. **41**, 1093–105 (1988).
2. Arbeit, R. D., Maki, D., Tally, F. P., Campanaro, E. & Eisenstein, B. I. The Safety And Efficacy Of Daptomycin For The Treatment Of Complicated Skin And Skin-Structure Infections. *Clin. Infect. Dis.* **38**, 1673–1681 (2004).
3. Fowler, V. G. *et al.* Daptomycin Versus Standard Therapy For Bacteremia And Endocarditis Caused By *Staphylococcus Aureus*. *N. Engl. J. Med.* **355**, 653–665 (2006).
4. Miller, W. R., Bayer, A. S. & Arias, C. A. Mechanism Of Action And Resistance To Daptomycin In *Staphylococcus Aureus* And Enterococci. *Cold Spring Harb. Perspect. Med.* **6**, a026997 (2016).
5. Friedman, L., Alder, J. D. & Silverman, J. A. Genetic Changes That Correlate With Reduced Susceptibility To Daptomycin In *Staphylococcus Aureus*. *Antimicrob. Agents Chemother.* **50**, 2137–2145 (2006).
6. Bayer, A. S. *et al.* Frequency And Distribution Of Single-Nucleotide Polymorphisms Within MprF In Methicillin-Resistant *Staphylococcus Aureus* Clinical Isolates And Their Role In Cross-Resistance To Daptomycin And Host Defense Antimicrobial Peptides. *Antimicrob. Agents Chemother.* **59**, 4930–4937 (2015).
7. Pader, V. *et al.* *Staphylococcus Aureus* Inactivates Daptomycin By Releasing Membrane Phospholipids. *Nat. Microbiol.* **2**, 16194 (2016).
8. Tran, T. T. *et al.* Daptomycin-Resistant *Enterococcus Faecalis* Diverts The Antibiotic Molecule From The Division Septum And Remodels Cell Membrane Phospholipids. *MBio* **4**, (2013).
9. Tran, T. T. *et al.* Mutations In CdsA And PgsA Correlate With Daptomycin Resistance In *Streptococcus Mitis* And *S. Oralis*. *Antimicrob. Agents Chemother.* **63**, e01531-18 (2018).
10. Goldner, N. K. *et al.* Mechanism Of High-Level Daptomycin Resistance In *Corynebacterium Striatum*. *mSphere* **3**, (2018).
11. Kleijn, L. H. J. *et al.* A High-Resolution Crystal Structure That Reveals Molecular Details Of Target Recognition By The Calcium-Dependent Lipopeptide Antibiotic Laspartomycin C. *Angew. Chemie Int. Ed.* **56**, 16546–16549 (2017).
12. Jung, D., Rozek, A., Okon, M. & Hancock, R. E. W. Structural Transitions As Determinants Of The Action Of The Calcium-Dependent Antibiotic Daptomycin. *Chem. Biol.* **11**, 949–957 (2004).
13. Jung, D., Powers, J. P., Straus, S. K. & Hancock, R. E. W. Lipid-Specific Binding Of The Calcium-

- Dependent Antibiotic Daptomycin Leads To Changes In Lipid Polymorphism Of Model Membranes. *Chem. Phys. Lipids* **154**, 120–128 (2008).
14. Muraih, J. K., Pearson, A., Silverman, J. & Palmer, M. Oligomerization Of Daptomycin On Membranes. *Biochim. Biophys. Acta - Biomembr.* **1808**, 1154–1160 (2011).
  15. Muraih, J. K., Harris, J., Taylor, S. D. & Palmer, M. Characterization Of Daptomycin Oligomerization With Perylene Excimer Fluorescence: Stoichiometric Binding Of Phosphatidylglycerol Triggers Oligomer Formation. *Biochim. Biophys. Acta - Biomembr.* **1818**, 673–678 (2012).
  16. Lee, M. T. *et al.* Molecular State Of The Membrane-Active Antibiotic Daptomycin. *Biophys. J.* **113**, 82–90 (2017).
  17. Lee, M. T. *et al.* Comparison Of The Effects Of Daptomycin On Bacterial And Model Membranes. *Biochemistry* **57**, 5629–5639 (2018).
  18. Zhang, T. *et al.* Cardiolipin Prevents Membrane Translocation And Permeabilization By Daptomycin. *J. Biol. Chem.* **289**, 11584–11591 (2014).
  19. Juhaniwicz-Dębińska, J., Dziubak, D. & Sęk, S. Physicochemical Characterization Of Daptomycin Interaction With Negatively Charged Lipid Membranes. *Langmuir* **36**, 5324–5335 (2020).
  20. Grein, F. *et al.* Ca<sup>2+</sup>-Daptomycin Targets Cell Wall Biosynthesis By Forming A Tripartite Complex With Undecaprenyl-Coupled Intermediates And Membrane Lipids. *Nat. Commun.* **11**, 1455 (2020).
  21. Kreuzberger, M. A., Pokorny, A. & Almeida, P. F. Daptomycin-Phosphatidylglycerol Domains In Lipid Membranes. *Langmuir* **33**, 13669–13679 (2017).
  22. Zhang, T. *et al.* Mutual Inhibition Through Hybrid Oligomer Formation Of Daptomycin And The Semisynthetic Lipopeptide Antibiotic CB-182,462. *Biochim. Biophys. Acta - Biomembr.* **1828**, 302–308 (2013).
  23. Taylor, R. *et al.* Two Successive Calcium-Dependent Transitions Mediate Membrane Binding And Oligomerization Of Daptomycin And The Related Antibiotic A54145. *Biochim. Biophys. Acta - Biomembr.* **1858**, 1999–2005 (2016).
  24. Zuttion, F. *et al.* High-Speed Atomic Force Microscopy Highlights New Molecular Mechanism Of Daptomycin Action. *Nat. Commun.* **11**, 6312 (2020).
  25. Mescola, A., Ragazzini, G. & Alessandrini, A. Daptomycin Strongly Affects The Phase Behavior Of Model Lipid Bilayers. *J. Phys. Chem. B* **124**, 8562–8571 (2020).
  26. Pogliano, J., Pogliano, N. & Silverman, J. A. Daptomycin-Mediated Reorganization Of Membrane Architecture Causes Mislocalization Of Essential Cell Division Proteins. *J. Bacteriol.* **194**, 4494–4504 (2012).
  27. Müller, A. *et al.* Daptomycin Inhibits Cell Envelope Synthesis By Interfering With Fluid Membrane Microdomains. *Proc. Natl. Acad. Sci. U. S. A.* **113**, E7077–E7086 (2016).
  28. Lam, H. Y. *et al.* Total Synthesis Of Daptomycin By Cyclization Via A Chemoselective Serine Ligation. *J. Am. Chem. Soc.* **135**, 6272–6279 (2013).
  29. Lohani, C. R., Taylor, R., Palmer, M. & Taylor, S. D. Solid-Phase Total Synthesis Of Daptomycin And Analogs. *Org. Lett.* **17**, 748–751 (2015).
  30. Wood, T. M. & Martin, N. I. The Calcium-Dependent Lipopeptide Antibiotics: Structure, Mechanism, & Medicinal Chemistry. *Med. Chem. Comm.* **10**, 634–646 (2019).
  31. Karas, J. A. *et al.* Structure–Activity Relationships Of Daptomycin Lipopeptides. *J. Med. Chem.* **63**,



- 13266–13290 (2020).
32. Chow, H. Y. *et al.* Establishing The Structure-Activity Relationship Of Daptomycin. *ACS Med. Chem. Lett.* **11**, 1442–1449 (2020).
  33. 't Hart, P. *et al.* A Combined Solid- And Solution-Phase Approach Provides Convenient Access To Analogues Of The Calcium-Dependent Lipopeptide Antibiotics. *Org. Biomol. Chem.* **12**, 913–918 (2014).
  34. Barnawi, G. *et al.* An Entirely Fmoc Solid Phase Approach To The Synthesis Of Daptomycin Analogs. *Pept. Sci.* **111**, e23094 (2019).
  35. Chow, H. Y. *et al.* Methylation Of Daptomycin Leading To The Discovery Of Kynomycin, A Cyclic Lipopeptide Active Against Resistant Pathogens. *J. Med. Chem.* **63**, 3161–3171 (2020).
  36. Sohlenkamp, C. & Geiger, O. Bacterial Membrane Lipids: Diversity In Structures And Pathways. *FEMS Microbiol. Rev.* **40**, 133–159 (2016).
  37. Müller, A., Klöckner, A. & Schneider, T. Targeting A Cell Wall Biosynthesis Hot Spot. *Nat. Prod. Rep.* **34**, 909–932 (2017).
  38. 't Hart, P., Oppedijk, S. F., Breukink, E. & Martin, N. I. New Insights Into Nisin's Antibacterial Mechanism Revealed By Binding Studies With Synthetic Lipid II Analogues. *Biochemistry* **55**, 232–237 (2016).
  39. Chiorean, S. *et al.* Dissecting The Binding Interactions Of Teixobactin With The Bacterial Cell-Wall Precursor Lipid II. *ChemBioChem* **21**, 789–792 (2020).
  40. Kleijn, L. H. J. *et al.* Total Synthesis Of Laspartomycin C And Characterization Of Its Antibacterial Mechanism Of Action. *J. Med. Chem.* **59**, 3569–3574 (2016).
  41. Koopmans, T. *et al.* Semisynthetic Lipopeptides Derived From Nisin Display Antibacterial Activity And Lipid II Binding On Par With That Of The Parent Compound. *J. Am. Chem. Soc.* **137**, 9382–9389 (2015).
  42. Wood, T. M., Bertheussen, K. & Martin, N. I. The Contribution Of Achiral Residues In The Laspartomycin Family Of Calcium-Dependent Lipopeptide Antibiotics. *Org. Biomol. Chem.* **18**, 514–517 (2020).
  43. Dong, Y. Y. *et al.* Structures Of DPAGT1 Explain Glycosylation Disease Mechanisms And Advance TB Antibiotic Design. *Cell* **175**, 1045–1058.e16 (2018).
  44. Cochrane, S. A. *et al.* Antimicrobial Lipopeptide Tridecaptin A 1 Selectively Binds To Gram-Negative Lipid II. *Proc. Natl. Acad. Sci.* **113**, 11561–11566 (2016).
  45. Turnbull, W. B. & Daranas, A. H. On The Value Of C: Can Low Affinity Systems Be Studied By Isothermal Titration Calorimetry? *J. Am. Chem. Soc.* **125**, 14859–14866 (2003).